

See discussions, stats, and author profiles for this publication at: <https://www.researchgate.net/publication/49621923>

Free-Standing Optical Gold Bowtie Nanoantenna with Variable Gap Size for Enhanced Raman Spectroscopy

ARTICLE *in* NANO LETTERS · NOVEMBER 2010

Impact Factor: 13.59 · DOI: 10.1021/nl102963g · Source: PubMed

CITATIONS

167

READS

242

8 AUTHORS, INCLUDING:



[Chun-Hway Hsueh](#)
National Taiwan University
240 PUBLICATIONS 4,560 CITATIONS

[SEE PROFILE](#)



[Gyula Eres](#)
Oak Ridge National Laboratory
134 PUBLICATIONS 3,094 CITATIONS

[SEE PROFILE](#)



[Zhenyu Zhang](#)
University of Science and Technology of C...
362 PUBLICATIONS 7,345 CITATIONS

[SEE PROFILE](#)



[Baohua Gu](#)
Oak Ridge National Laboratory
160 PUBLICATIONS 6,696 CITATIONS

[SEE PROFILE](#)

Free-Standing Optical Gold Bowtie Nanoantenna with Variable Gap Size for Enhanced Raman Spectroscopy

Nahla A. Hatab,[†] Chun-Hway Hsueh,^{‡,||,⊥} Abigail L. Gaddis,[‡] Scott T. Retterer,[§] Jia-Han Li,[¶] Gyula Eres,[‡] Zhenyu Zhang,^{*,‡,||} and Baohua Gu^{*,†}

[†] Environmental Sciences, [‡] Materials Science and Technology Divisions, and [§] Center for Nanophase Materials Sciences, Oak Ridge National Laboratory, Oak Ridge, Tennessee 37831, United States, ^{||} Department of Physics and Astronomy, University of Tennessee, Knoxville, Tennessee 37996, United States, and [⊥] Department of Materials Science and Engineering and [¶] Department of Engineering Science and Ocean Engineering, National Taiwan University, Taipei 106, Taiwan

ABSTRACT We describe plasmonic interactions in suspended gold bowtie nanoantenna leading to strong electromagnetic field (*E*) enhancements. Surface-enhanced Raman scattering (SERS) was used to demonstrate the performance of the nanoantenna. In addition to the well-known gap size dependence, up to 2 orders of magnitude additional enhancement is observed with elevated bowties. The overall behavior is described by a SERS enhancement factor exceeding 10^{11} along with an anomalously weak power law dependence of *E* on the gap size in a range from 8 to 50 nm that is attributed to a plasmonic nanocavity effect occurring when the plasmonic interactions enter a strongly coupled regime.

KEYWORDS Electron beam lithography, FDTD simulation, optical nanoantenna, single molecule SERS, collective photonic effect

It is now widely recognized that the extreme sensitivity of SERS is dominated by the electromagnetic enhancement, referring to the intense, spatially varying *E* fields produced by plasmonic coupling between closely spaced metal nanoparticles.^{1–15} A particularly intriguing feature of the electromagnetic enhancement is associated with the presence of the so-called “nanogap” effect where local SERS enhancement factors (EF) sufficient for detection of single molecules have been observed.^{1,2} Theoretical analysis using model systems consisting of closely spaced metal nanostructures have identified the size, shape, gap distance, the wavelength and polarization of the incident light as key factors that govern the overall EF within the nanogap.^{1–5,16–18} These advances in understanding the nanogap effect motivated new experimental approaches that, instead of searching for isolated hot spots or nanogaps in random nanoparticle aggregates,^{19,20} use electron beam lithography (EBL) fabricated periodic nanostructures.^{3,5,21} EBL is the ideal tool for fabricating SERS substrates with precisely defined shape and systematically variable nanogap size necessary for gaining insight into the underlying enhancement mechanisms and for achieving maximal enhancement. Recent compelling examples include the demonstration of a strong polarization and gap size dependent response from single gold nanobowties fabricated by EBL,^{3,7} and the high-

harmonic generation by resonant plasmon field enhancement from a closely packed gold bowtie arrays.²² However, the large enhancement factors expected to occur for gap sizes on the order of a few nanometers remain difficult to confirm^{3–5,7,23} primarily because the resolution necessary for generating such features is beyond the capabilities of conventional EBL.^{3,7,15} Overcoming these technical hurdles promises advances in fundamental understanding of gap-dependent *E* field coupling that enable design and fabrication of a new generation of nanostructures that are capable of reliably and reproducibly performing single molecule detection and spectroscopy, and advanced optoelectronic functionality.^{5,14,15}

Here we demonstrate large SERS enhancement factors exceeding 10^{11} resulting from a new configuration of elevated gold bowtie nanoantenna arrays with optimized array periodicity. Figure 1a shows a schematic illustration of these structures, together with a scanning electron microscope (SEM) image of the actual structures in Figure 1b, and the spatial distribution of the *E* field intensity calculated by finite difference time domain (FDTD) simulations shown in Figure 1c. A process combining nanofabrication steps of pattern definition by EBL, metal deposition, liftoff, and reactive ion etching (RIE) arranged in a particular sequence was used to fabricate the elevated gold bowtie arrays on Si wafers according to details given in Supporting Information. A precisely controlled deposition of 40 nm gold on a Cr adhesion layer located on top of 200 nm tall Si posts was used to close the 20 nm gap size defined by EBL to 8 ± 1 nm. This step also produces the characteristic overhang that

* To whom correspondence should be addressed. E-mail: (B.G.) gub1@ornl.gov; (Z.Z.) zhangz@ornl.gov.

Received for review: 08/21/2010

Published on Web: 11/19/2010

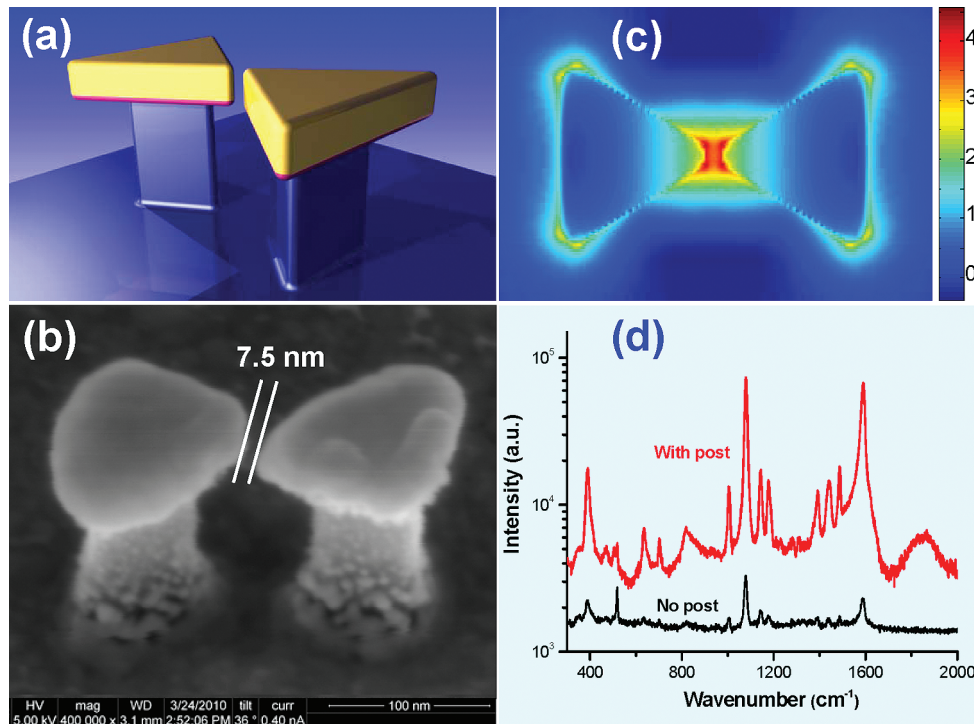


FIGURE 1. (a) Schematic illustration of elevated gold bowties on top of Si posts etched into a Si wafer with a magenta colored Cr adhesion layer between the gold layer and the Si post. (b) Side view SEM image of a three-dimensional gold bowtie nanoantenna with a gap of 8 ± 1 nm. (c) The spatial distribution of the E field intensity calculated by FDTD simulations for bowtie equilateral triangle sides of 100 nm, gap size of 10 nm, Si posts of 40 nm in diameter and 200 nm in height, and an apex width of 10 nm (see Supporting Information Figure S3). The intensity is given by a logarithmic scale color bar. (d) Comparison of SERS spectra of *p*-mercaptoaniline from elevated and nonelevated bowtie array substrates.

along with the post defines the three-dimensional nanoantenna (Figure 1b) and distinguishes these structures from gold bowties that remain attached to the substrate.^{3,7,21,22} The contrast in SEM backscattered electron images (Supporting Information Figure S1) shows that only the bowties and not the posts are coated with gold. A comparison of SERS spectra of elevated bowties with that of bowties attached to the substrate is shown in Figure 1d. The elevated bowties allow manifestation of intrinsic plasmonic coupling effects in suspended nanocavities, or the tip-to-tip nanogaps, from structures that are not in physical contact with a substrate. This configuration results in up to 2 orders of magnitude additional enhancement in SERS response compared to that of nonelevated bowtie arrays (Figure 1d). The influence of the post heights on the SERS response is confirmed by and qualitatively agrees with FDTD simulation results illustrated in Supporting Information Figure S4. Experimental studies of SERS dependence on the post height are the subject of ongoing work and will be described in a future publication.

Different density arrays shown in Figure 2a were fabricated by changing the center-to-center distance (ccd) in rows along the bowtie axis, and the row-to-row distance (rrd). The isolated bowtie arrays shown in image II of Figure 2a have a dimension of $\text{ccd} = \text{rrd} = 2 \mu\text{m}$ that is close to the laser spot size, which ensures that the SERS measurements represent local response from a single bowtie. We next

compare the SERS response of isolated bowties with that from high-density (III) and low-density (I) arrays in Figure 2a with specific periodicity of $\text{ccd} = \text{rrd} = 300 \text{ nm}$, and $\text{ccd} = 785 \text{ nm}$, $\text{rrd} = 2 \mu\text{m}$, respectively. The Raman EF for these arrays shown in Figure 2b was determined from the SERS intensity of a probing molecule, *p*-mercaptoaniline (*p*MA).^{6,24} Exposure of the bowties to a *p*MA solution (10^{-5} M) results in the chemisorption and uniform coating of the gold surface by a monolayer of *p*MA molecules that ensures unambiguous determination of the SERS enhancement and good reproducibility (Supporting Information Figure S2). The EF was determined following a procedure established in the literature^{3,6,24–26} and is described in Supporting Information. Here the EF represents the ratio of the SERS signal to the nonenhanced bulk Raman signal measured and normalized per molecule for the 1588 cm^{-1} Raman band.

For all arrays, the EF increases with decreasing gap size and reaches 2×10^{11} and 7×10^{11} at the smallest gap of $8 \pm 1 \text{ nm}$ for the isolated and low-density bowtie arrays (Figure 2b). These values match the largest enhancements reported for nanoshells and nanoparticle aggregates that typically contain a number of randomly distributed hot spots.^{6,19,20,24} In addition to the distinct gap size dependence that dominates the response of isolated bowties, we demonstrate that the bowtie arrays are also subject to collective interactions that either degrade or further enhance the overall SERS response. The trends in Figure 2b identify the

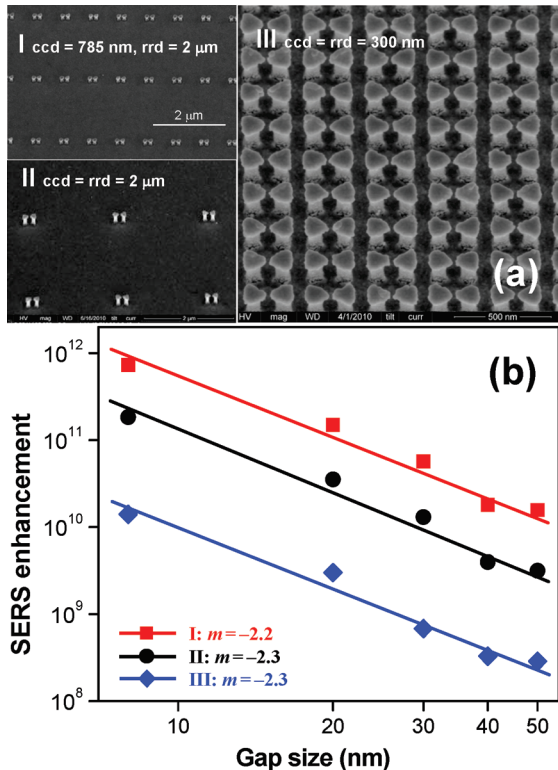


FIGURE 2. Determination of the gap size dependence and the long-range collective plasmonic effects in SERS enhancement using elevated gold bowtie nanoantenna arrays. (a) SEM images of the elevated gold bowtie arrays with varying center-to-center distance in rows along the bowtie axis, and row-to-row distance. (b) A log-log plot of SERS enhancement factors as a function of bowtie nanogap size in arrays I, II, and III with different bowtie spacing. The slope is determined by fitting the power-law relationship of $\text{EF} \propto Ad^m$ to the experimental data.

array periodicity as the critical factor that determines the EF change. The maximal enhancement is achieved when the periodicity of the arrays matches the laser wavelength. In particular, we note that the EF from the high-density bowtie array with $ccd = rrd = 300 \text{ nm}$ (III in Figure 2) was about 1 order of magnitude lower than that for the isolated bowties. In contrast, the low-density arrays with optimized periodicity of $ccd = 785 \text{ nm}$ (I in Figure 2) that matches the Raman laser wavelength, produced an EF with nearly an order of magnitude additional increase above that for isolated bowties. These observations represent the first definitive experimental confirmation of the theoretically predicted long-range collective photonic effect.^{16,17,27} This important finding suggests that even greater enhancements might have been realized in previous experiments^{12,22} had the bowtie or nanoparticle arrays been more sparsely distributed.

The FDTD simulations identify the shape and sharpness (w) of the triangle's apex (Supporting Information Figure S3) as factors that affect efficient coupling of the incident optical radiation into the bowtie gap. The spatial distribution plot of the E field intensity in Figure 1c shows that for elevated bowties the nanogap effect is strongly localized in the volume between the tips of the triangles. In addition, Figure

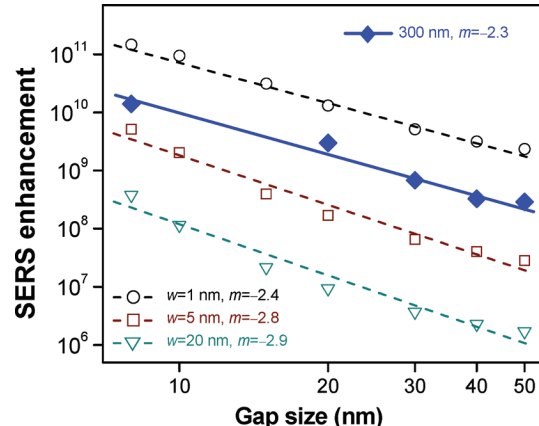


FIGURE 3. Comparison of the FDTD calculated maximum field $|E|^4$ enhancement (dashed lines with open symbols) for apex widths $w = 1, 5, \text{ and } 20 \text{ nm}$ with the experimentally determined SERS enhancement (solid line with solid diamonds) as a function of nanogap size for elevated bowtie arrays with $ccd = rrd = 300 \text{ nm}$ (III in Figure 2). The slope is determined by fitting the power-law relationship of $\text{EF} \propto |E|^4 = Ad^m$ to the data.

3 illustrates that the nanogap effect and the resulting SERS response become stronger with the apex sharpness (w) increasing from 20 to 1 nm.

The elevated gold bowtie arrays reveal another important feature of the EF. A log-log plot of the EF against the gap size, d , gives a straight line with a slope (m) near -2.2 ± 0.1 for the bowtie arrays (Figure 2b). Similar magnitude and slope are obtained using FDTD simulations for the high-density bowtie arrays with apex width near 1 nm (Figure 3). On the basis of the general relationship of the EF $\propto |E|^4 = Ad^m$, this behavior is equivalent to a weak power law dependence of E on the gap size given by $E \sim d^{-0.56}$, that is even weaker than the decay of a monopole field according to Coulomb's law of $E \sim d^{-2}$. These findings suggest that narrowing the gap separation between the two prisms below $\sim 50 \text{ nm}$ the bowties enter into a regime characterized by exceptionally strong E field within the gap region. In this strongly coupled regime, the E field shows little attenuation possibly due to resonant nanocavity effects²⁸ supported by both experimental observations and the FDTD simulation (Supporting Information Figure S5). However, the weak power law dependence may also include a component resulting from red shifting of the plasmon resonant frequency with decreasing gap size.^{17,29,30} According to the plasmon ruler equation^{31,32} the plasmon wavelength shift reaches maximum for very small gap sizes and decays exponentially with the gap size. Nevertheless, an important technological significance of this weak attenuation comes with the realization that in the strong coupling regime the arrays can tolerate a certain degree of gap size nonuniformity and geometrical imperfection without losing their ability for large field enhancement. The spatial localization of a free-standing, finite plasmonic volume enabled by the three-dimensional suspended bowtie nanoantenna substantially expands the versatility of utilizing E -field enhancement

that has numerous applications in chemistry and physics including single molecule spectroscopy, and a variety of advanced optical characterization, manipulation, and optical information processing using periodic metallic nanostructures.

Acknowledgment. We thank C.M. Rouleau for his contribution to the art work in this paper. This work was supported by the Strategic Environmental Research and Development Program (SERDP) of the U.S. Department of Defense (N.A.H. and B.G.), the Materials Sciences and Engineering Division, Office of Basic Energy Sciences, U.S. Department of Energy (DOE) (A.L.G., G.E., and Z.Z.), and the National Science Council of Taiwan (C.H. and J.L.). The fabrication of the gold bowtie nanoantenna was conducted at the Center for Nanophase Materials Sciences of Oak Ridge National Laboratory (ORNL), which is sponsored by DOE Scientific User Facilities Division (S.T.R.). ORNL is managed by UT-Battelle, LLC, for U.S. DOE under contract DE-AC05-00OR22725.

Supporting Information Available. Fabrication of elevated gold bowtie arrays on silicon wafers, sample characterization and Raman spectroscopic analysis, determination of SERS enhancement factors, FDTD computational algorithm and model simulations, additional figures, and additional references. This material is available free of charge via the Internet at <http://pubs.acs.org>.

REFERENCES AND NOTES

- (1) Xu, H.; Bjerneld, E. J.; Kall, M.; Borjesson, L. *Phys. Rev. Lett.* **1999**, *83*, 4357–4360.
- (2) Michaels, A. M.; Jiang, J.; Brus, L. *J. Phys. Chem. B* **2000**, *104* (50), 11965–11971.
- (3) Fromm, D. P.; Sundaramurthy, A.; Schuck, P. J.; Kino, G.; Moerner, W. E. *Nano Lett.* **2004**, *4* (5), 957–961.
- (4) Wang, H.; Levin, C. S.; Halas, N. J. *J. Am. Chem. Soc.* **2005**, *127* (43), 14992–14993.
- (5) Qin, L. D.; Zou, S. L.; Xue, C.; Atkinson, A.; Schatz, G. C.; Mirkin, C. A. *Proc. Natl. Acad. Sci. U.S.A.* **2006**, *103* (36), 13300–13303.
- (6) Haynes, C. L.; Van Duyne, R. P. *J. Phys. Chem. B* **2003**, *107* (30), 7426–7433.
- (7) Fromm, D. P.; Sundaramurthy, A.; Kinkhabwala, A.; Schuck, P. J.; Kino, G. S.; Moerner, W. E. *J. Chem. Phys.* **2006**, *124* (6), No. 061101.
- (8) Dieringer, J. A.; Lettan, R. B.; Scheidt, K. A.; Van Duyne, R. P. *J. Am. Chem. Soc.* **2007**, *129* (51), 16249–16256.
- (9) Etchegoin, P. G.; Le Ru, E. C. *Phys. Chem. Chem. Phys.* **2008**, *10* (40), 6079–6089.
- (10) Camden, J. P.; Dieringer, J. A.; Wang, Y. M.; Masiello, D. J.; Marks, L. D.; Schatz, G. C.; Van Duyne, R. P. *J. Am. Chem. Soc.* **2008**, *130* (38), 12616.
- (11) Qian, X. M.; Nie, S. M. *Chem. Soc. Rev.* **2008**, *37* (5), 912–920.
- (12) Fang, Y.; Seong, N. H.; Dlott, D. D. *Science* **2008**, *321* (5887), 388–392.
- (13) Li, J. F.; Huang, Y. F.; Ding, Y.; Yang, Z. L.; Li, S. B.; Zhou, X. S.; Fan, F. R.; Zhang, W.; Zhou, Z. Y.; Wu, D. Y.; Ren, B.; Wang, Z. L.; Tian, Z. Q. *Nature* **2010**, *464* (7287), 392–395.
- (14) Lim, D. K.; Jeon, K. S.; Kim, H. M.; Nam, J. M.; Suh, Y. D. *Nat. Mater.* **2010**, *9* (1), 60–67.
- (15) Theiss, J.; Pavaskar, P.; Echternach, P. M.; Muller, R. E.; Cronin, S. B. *Nano Lett.* **2010**, *10*, 2749–2754.
- (16) Zou, S. L.; Schatz, G. C. *Chem. Phys. Lett.* **2005**, *403* (1–3), 62–67.
- (17) Zhao, K.; Xu, H.; Gu, B.; Zhang, Z. *J. Chem. Phys.* **2006**, *125*, No. 081102.
- (18) Tabor, C.; Murali, R.; Mahmoud, M.; El-Sayed, M. A. *J. Phys. Chem. A* **2009**, *113* (10), 1946–1953.
- (19) Kneipp, K.; Wang, Y.; Kneipp, H.; Perelman, L. T.; Itzkan, I.; Dasari, R.; Feld, M. S. *Phys. Rev. Lett.* **1997**, *78* (9), 1667–1670.
- (20) Nie, S.; Emory, S. R. *Science* **1997**, *275*, 1102–1106.
- (21) Kinkhabwala, A.; Yu, Z. F.; Fan, S. H.; Avlasevich, Y.; Mullen, K.; Moerner, W. E. *Nat. Photonics* **2009**, *3* (11), 654–657.
- (22) Kim, S.; Jin, J. H.; Kim, Y. J.; Park, I. Y.; Kim, Y.; Kim, S. W. *Nature* **2008**, *453*, 757–760.
- (23) Hinde, R. J.; Sepaniak, M. J.; Compton, R. N.; Nordling, J.; Lavrik, N. *Chem. Phys. Lett.* **2001**, *339* (3–4), 167–173.
- (24) Jackson, J. B.; Halas, N. J. *Proc. Natl. Acad. Sci. U.S.A.* **2004**, *101* (52), 17930–17935.
- (25) Hu, X. G.; Wang, T.; Wang, L.; Dong, S. J. *J. Phys. Chem. C* **2007**, *111* (19), 6962–6969.
- (26) Wells, S. M.; Retterer, S. D.; Oran, J. M.; Sepaniak, M. J. *ACS Nano* **2009**, *3* (12), 3845–3853.
- (27) Haynes, C. L.; McFarland, A. D.; Zhao, L. L.; Van Duyne, R. P.; Schatz, G. C.; Gunnarsson, L.; Prikulis, J.; Kasemo, B.; Kall, M. *J. Phys. Chem. B* **2003**, *107* (30), 7337–7342.
- (28) Dong, Z. C.; Zhang, X. L.; Gao, H. Y.; Luo, Y.; Zhang, C.; Chen, L. G.; Zhang, R.; Tao, X.; Zhang, Y.; Yang, J. L.; Hou, J. G. *Nat. Photonics* **2010**, *4* (1), 50–54.
- (29) Sundaramurthy, A.; Crozier, K. B.; Kino, G. S.; Fromm, D. P.; Schuck, P. J.; Moerner, W. E. *Phys. Rev. B* **2005**, *72* (16), 1098–0121.
- (30) Zhao, L. L.; Kelly, K. L.; Schatz, G. C. *J. Phys. Chem. B* **2003**, *107* (30), 7343–7350.
- (31) Jain, P. K.; Huang, W. Y.; El-Sayed, M. A. *Nano Lett.* **2007**, *7* (7), 2080–2088.
- (32) Zuloaga, J.; Prodan, E.; Nordlander, P. *Nano Lett.* **2009**, *9* (2), 887–891.